


RESEARCH PAPER

OPEN ACCESS 

Protective effect of miR-33-5p on the M1/M2 polarization of microglia and the underlying mechanism

Song Chai^{a,†}, Yilan Sheng^{a,b,†}, Ran Sun^a, Jieshi He^c, Lihua Chen^d, Fei He^a, Wenhua Chen^{a,b}, Dingying Ma^c, and Bo Yu^{a,b}

^aDepartment of Rehabilitation Medicine, Shanghai General Hospital, Shanghai Jiaotong University, Shanghai, China; ^bDepartment of Rehabilitation, School of International Medical Technology, Shanghai Sanda University, Shanghai, Pudong, China; ^cDepartment of Rehabilitation Medicine, Ningbo No. 9 Hospital, Ningbo, Zhejiang Province, China; ^dDepartment of Rehabilitation, Shanghai Fifth Rehabilitation Hospital, Shanghai, China

ABSTRACT

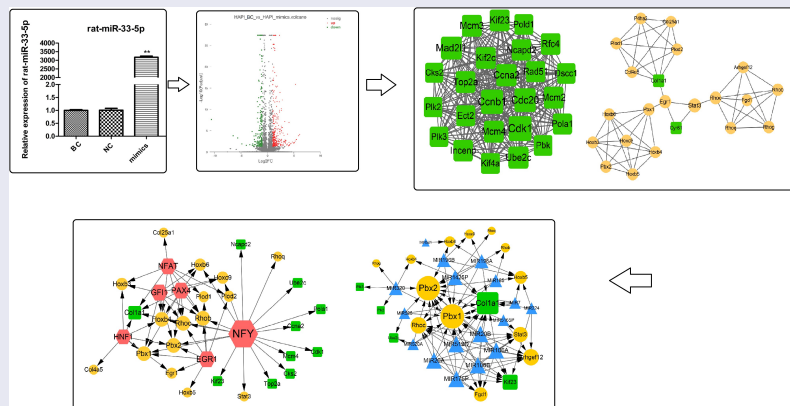
This study was aimed to investigate the influence of miR-33-5p on the M1/M2 polarization of microglia and the underlying mechanism. Transcriptome sequencing was performed using microglia from miR-33-5p mimic and control groups. In total, 507 differentially expressed genes, including 314 upregulated genes and 193 downregulated genes, were identified. The subnetwork of module A, which was extracted from the protein–protein interaction networks, mainly contained the downregulated genes. *Cdk1*, *Ccnb*, and *Cdc20*, the members of module-A networks with the highest degrees, possess the potential of being biomarkers of ischemic stroke due to their function in the cell cycle. NFY, a transcription factor, was predicted to have the regulatory relation with nine downregulated genes. Overall, our findings will provide a valuable foundation for genetic mechanisms and treatment studies of ischemic stroke.

ARTICLE HISTORY

Received 19 January 2022
Revised 16 March 2022
Accepted 25 March 2022

KEYWORDS

Microglia; transcript sequencing; M1/M2 polarization







Highlights

- PCA analysis showed significant differences between HAPI-mimic and blankcontrol groups.
- Cell cycle-related genes, such as *Cdk1*, *Ccnb1*, and *Cdc20*, were identified based on modularized genes.

- The transcription factor NFY regulated nine downregulated genes.

Introduction

Cardiovascular and cerebrovascular diseases are common and serious threats to humans worldwide [1]. Approximately 80 million people have experi-

CONTACT Dingying Ma  dingyingma@163.com  Department of Rehabilitation Medicine Ningbo No. 9 Hospital, Ningbo, Zhejiang Province, China
Bo Yu  Boyujtu@163.com  Department of Rehabilitation Medicine, Shanghai General Hospital, Shanghai Jiao Tong University, No. 100, Haining Road, Shanghai, 200080, China.

[†]Song Chai and Yilan Sheng should be regarded as co-first authors.

© 2022 The Author(s). Published by Informa UK Limited, trading as Taylor & Francis Group.

This is an Open Access article distributed under the terms of the Creative Commons Attribution License (<http://creativecommons.org/licenses/by/4.0/>), which permits unrestricted use, distribution, and reproduction in any medium, provided the original work is properly cited.

enced stroke, and more than 50 million survivors suffer from some form of permanent disability. Cerebral apoplexy is divided into ischemic stroke and hemorrhagic stroke, among which ischemic stroke is the most common [2]. The morbidity, mortality, and recurrence rate of ischemic stroke are extremely high [3]. The pathophysiological basis of ischemic stroke includes cell apoptosis, imbalance in body oxidation and antioxidation, toxicity effects of excitatory amino acids, and cell inflammation [4]. In many neurodegenerative diseases, the inflammatory response is closely related to the activation and polarization of microglia [5], a group of inflammatory cells [6].

Microglia are the smallest cells in the central nervous system, with small nuclei and little cytoplasm [7]. Microglia are mainly concentrated in the telencephalon, basal ganglia, olfactory bulb, and hippocampus, and are the brain's inherent immune effector cells, participating in dynamic balance and host defense against pathogens and central nervous system diseases [8]. Microglia are activated under pathological conditions, which are named polarization of microglia [9]. Microglial activation is divided into two major phenotypes: classical activation (also known as M1 phenotype) and substitution activation (M2 phenotype) [10]. M1-type microglia is associated with cytotoxicity, superoxide production, and cytokine secretion [11]. The factors released by M1 microglial cells can inhibit tissue repair, destroy the blood-brain barrier, and participate in neuronal degeneration [12]. In contrast to the M1 phenotype, the M2 microglial phenotype exerts anti-inflammatory effects and promotes wound healing and tissue repair. M2-type microglia can also promote the expression of neuroprotective factors and participate in tissue repair and remodeling by changing gene expression [13]. Therefore, it is of great value to inhibit common markers on the surface of M1 microglia to reduce the cytotoxic effect and enhance the beneficial effect of M2 microglia [14]. However, the mechanism of M1/M2 polarization in microglia remains unclear.

MiR-33-5p has been shown to play a crucial role in the inflammatory response [15], macrophage lipid accumulation [16], and cell proliferation [17]. Zeng et al. demonstrated that miR-33-5p

may be a potential biomarker for acute ischemic stroke [18]. Direct intracerebral delivery of miR-33 also changed gene expression [19]. Nevertheless, whether miR-33 is associated with the M1/M2 polarization of microglia and thus indirectly participates in the occurrence of ischemic stroke is still unknown.

As a result, this study was aimed to investigate the influence of miR-33-5p on the M1/M2 polarization of microglia and the underlying mechanism. The changes in gene expression after miR-33-5p overexpression were analyzed by RNA sequencing and bioinformatics methods. Western blotting was used to verify the results.

Materials and methods

Cell culture and transfection

Rat microglial HAPI cells were purchased from BNCC (Art. No. BNCC340723, Beijing, China). Briefly, HAPI cells were cultured in Roswell Park Memorial Institute (RPMI) 1640 medium with 10% fetal bovine serum at 37°C and 5% CO₂ in an incubator.

HAPI cells, at ~80% confluence, were harvested using a trypsin detachment solution and inoculated into a 6-well plate at a density of 5×10^5 cells/well. Cells were transfected with miR-33-5p mimics according to the manufacturer's instructions (GenePharma Co., Ltd, Shanghai, China). After 48 h of transfection, the cell precipitate was collected and lysed with 1 mL TRIzol for qPCR detection.

Real-time PCR

Real-time PCR was performed as described previously [20]. Briefly, the reverse transcription system contained 4 μ L 5 \times primeScript RT Master MIX (perfect Real Time), 1 μ g RNA, and 15 μ L RNase Free water (up to 20 μ L). RT-PCR was performed using a quantitative PCR (ABI 7500, Thermo Fisher Scientific, MA, USA) in the presence of a fluorescent dye (SYBR Green I; Takara, NJ, USA). The primers used in this study are shown in Table 1.

Table 1. The primers used in this study.

Primers	Sequences (5'-3')
rat-miR-33-5p-F	AGCTCGGTGATTGTAGTTGC
rat-miR-33-5p-R	GTGCAGGGTCCGAGGT
rat-U6-F	GCTTCGGCAGCACATATACTAAAAT
rat-U6-R	CGCTTCACGAATTTGCGTGTCTAT
β-actin-rat-F	ATTGCTGACAGGATGCAGAA
β-actin-rat-R	TAGAGCCACCAATCCACACAG
rat-CCL2-F	ACCAGCAGCAGGTGTCCCA
rat-CCL2-R	TGCTTGAGGTGGTTGTGGAA
rat-IL-1β-F	CAGGATGAGGACCAAGCAC
rat-IL-1β-R	GTGAGCAGCAGCAGGACATT
rat-TNF-α-F	GCCTCTTCTCATTCTGCTCG
rat-TNF-α-R	TCCGCTTGGTGGTTGTCTAC
rat-Ym-1-F	TGGAGGCTGGAAGTTTGGAT
rat-Ym-1-R	GATGAATGTCTGCCGTTCTG
rat-CD206-F	GTGCCTACTGCCTGCCCTAA
rat-CD206-R	TCCCATCGCTCCACTCAAAG
rat-Arg1-F	GAGAAAGGTCCCGCAGCAT
rat-Arg1-R	CAGACCGTGGGTTCTTCACAA
rat-Slc7a5-F	TGGAGCGTCCCATCAAGGT
rat-Slc7a5-R	GAGCACGGTCCCGGAGAAGA
rat-Rhob-F	CTCGGCCAAGACCAAGGAG
Rat-Rhob-R	AGCAGTTGATGCAGCCATTCT
rat-Smad1-F	CAGCGTGTGGTGGATGGT
rat-Smad1-R	TCACTGAGGCACTCCGCATA
rat-Rhog-F	CGACCGTGAACCTAAACCT
rat-Rhog-R	GTGGACTGGCAATGGAGAAAC
rat-Mybl2-F	TTGTGGATGAGGATGGGAAGA
rat-Mybl2-R	CCTGGTTGAGCAGGCTGTTAT
rat-GAPDH-F	AGACAGCCGCATCTTCTGT
rat-GAPDH-R	CTGCCGTGGGTAGAGTCAT

Table 2. Pathways and BP terms (top 5) enriched by upregulated DEGs.

Category	Term	Count	PValue
PATHWAY	mo04010:MAPK signaling pathway	12	5.16E-03
PATHWAY	mo05202:Transcriptional misregulation in cancer	9	9.38E-03
PATHWAY	mo00500:Starch and sucrose metabolism	4	1.25E-02
PATHWAY	mo04213:Longevity regulating pathway – multiple species	5	1.63E-02
PATHWAY	mo05135:Yersinia infection	7	1.72E-02
GO_BP	GO:0045944~ positive regulation of transcription from RNA polymerase II promoter	42	7.89E-07
GO_BP	GO:0006357~ regulation of transcription from RNA polymerase II promoter	44	6.59E-06
GO_BP	GO:0048704~ embryonic skeletal system morphogenesis	8	2.44E-05
GO_BP	GO:0007399~ nervous system development	14	4.30E-05
GO_BP	GO:0086010~ membrane depolarization during action potential	5	6.75E-05

Western blotting

After lysis with RIPA lysis buffer, proteins were extracted from the fully lysed sample. Proteins from each sample were separated by sodium

dodecyl sulfate (SDS)-polyacrylamide gel electrophoresis and transferred to a PVDF membrane. After transfer, the membranes were incubated with 5% skim milk. Then, the blots were washed thrice with 1× PBS-T (1000 mL 1× PBS + 1 mL Tween-20) for 5–10 min. The primary antibody diluted with 5% skim milk was incubated overnight at 4°C. After washing the membrane six times, secondary antibody was added and transferred to a table concentrator at 37°C for 2 h. Finally, bands were detected using the Millipore ECL system. Tanon Image Software was used for grayscale analysis. $P < 0.05$ was the screening criterion for significant difference.

cDNA library construction and transcriptome sequencing

The sequencing experiment was performed using the Illumina Truseq™ RNA sample prep Kit method for library construction. Briefly, total RNA was extracted using TRIzol reagent (Invitrogen) and its concentration and purity were detected using Nanodrop 2000. After reverse transcription, jointing adaptor, and PCR amplification, a cDNA library was constructed. The library was sequenced using an Illumina HiSeq™ 2000 sequencer (Illumina, San Diego, CA, USA).

Raw reads filtering

To ensure the accuracy of the subsequent analysis, the original sequencing data were filtered by removing joint sequences, low-quality read segments, and high N (N represents uncertain base information) rate sequence. SeqPrep [21] and Sickle [22] were used to remove the joint sequence from reads, sequences of less than 50 bp, and low-quality sequences.

Mapping and differential expression analysis

Based on the clean data, TopHat2 [23] was used to perform a sequence alignment analysis. Based on the existing reference genome, the mapped reads were assembled and spliced to obtain differentially expressed genes (DEGs) and new transcripts using Cufflinks [24] and StringTie [25]. The screening

criteria for DEGs were $|\log(\text{FC})| > 1$ and p-value < 0.05 .

Functional enrichment analysis of differentially expressed genes (DEGs)

The DEGs were subjected to Gene Ontology (biological process; GO BP) and Kyoto Encyclopedia of Genes and Genomes (KEGG) annotation using the common enrichment analysis tool DAVID [26] (version 6.8). The thresholds were count ≥ 2 and p-value < 0.05 .

Construction of a protein–protein interaction (PPI) network of DEGs

The interaction relationship between DEG-coding proteins was predicted and analyzed using the STRING [27] (version 10.0) database (PPI score: 0.15). Cytoscape plugin MCODE (version 1.4.2) was used to analyze the module in the PPI network (score > 5).

Additionally, the module genes were mapped using GO BP and KEGG databases for functional annotation. DAVID [26] (version 6.8) was used to perform the function analyses, with thresholds of count ≥ 2 and p-value < 0.05 .

Transcription Factor (TF)-target and miRNA-target regulatory network prediction

Based on the significant module genes, the Overrepresentation Enrichment Analysis (ORA) method in WebGestalt [28] was used to predict the TF-target and miRNA-target regulatory relation for network construction.

Statistical analysis

All experiments were repeated three times. Data are shown as mean \pm standard deviation. GraphPad Prism 5 (San Diego, CA, USA) was used to analyze the data from this study. One-way analysis of variance was used for comparisons among groups, followed by Newman-Keuls multiple comparison test. Statistical significance was considered for p-values less than 0.05.

Results

Expression of miR-33-5p and M1/M2 biomarkers

The expression level of miR-33-5p was detected by RT-PCR. As shown in Figure 1(a), the expression of miR-33-5p in the mimic group was significantly higher than that in the blank control (BC) and negative control (NC) groups ($p < 0.01$). The biomarkers of M1 microglia (*CCL2*, *IL-1*, and *TNF- α*) and biomarkers of M2 microglia (*Ym-1*, *CD206*, and *Arg1*) were detected. The expression levels of the three biomarker genes of M1 in the mimic group were significantly increased compared with those in the BC and NC groups, while M2 in the mimic group were significantly reduced compared with those in the BC and NC groups (Figure 1(b)).

Genes differentially expressed upon miR-33-5p overexpression

To investigate the action mechanism of miR-33-5p in the M1/M2 polarization of microglia, DEGs between the groups with or without miR-33-5p mimic treatment were identified. In total, 507 DEGs were found, which included 314 upregulated genes and 193 downregulated genes. The heatmap and volcano plot of DEGs are shown in Figure 2(a-b).

Functional enrichment analysis of differentially expressed genes (DEGs)

The upregulated DEGs were significantly enriched in 84 BP terms, such as positive regulation of transcription from RNA polymerase II promoter, and regulation of transcription from RNA polymerase II promoter, and 6 KEGG pathways, such as MAPK signaling pathway and transcriptional misregulation in cancer. The downregulated DEGs were significantly enriched in 59 BP terms, such as, mitotic DNA replication initiation, and DNA unwinding involved in DNA replication, and 8 KEGG pathways, such as cell cycle, and DNA replication. The top 5 terms for the enrichment results are shown in Tables 2 and 3.

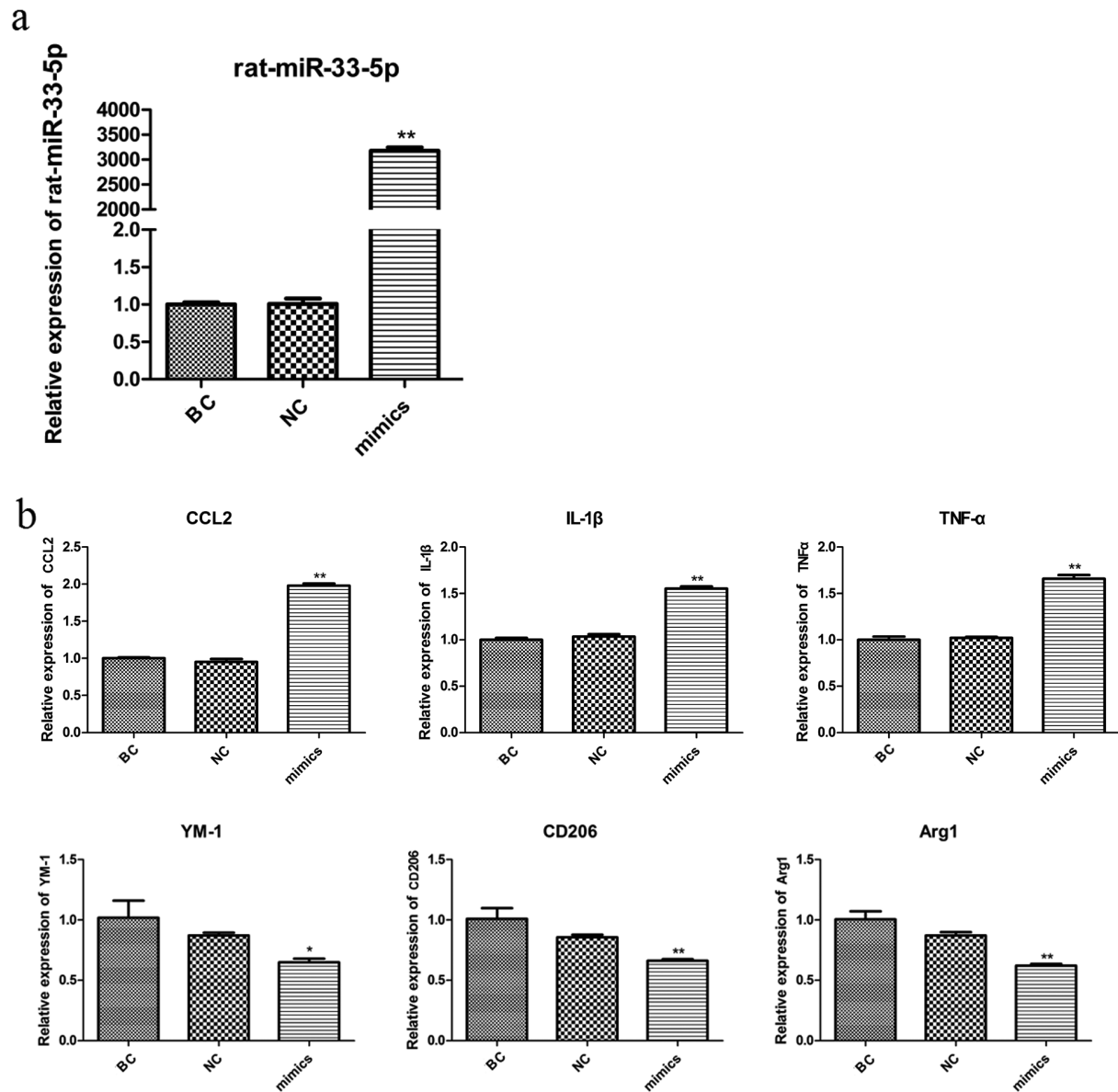


Figure 1. The expression of miR-33-5p (a) and biomarkers of M1/M2 microglia (b). * $p < 0.05$ and ** $p < 0.01$.

Protein–protein interaction (PPI) network and module analysis

To obtain more interactions, PPI networks were constructed using STRING. As shown in Figure 3, 407 nodes and 1347 edges were included in the networks. The top ten nodes, with higher degrees, were *Cdk1*, *Ccnb1*, *Cdc20*, *Mad2l1*, *Ccna2*, *Ube2c*, *Mcm3*, *Mcm4*, *Kif2c*, and *Kif23*. Due to the large number of nodes in the network, we further selected the key module from the network. Two modules were finally obtained with the threshold of score > 5 , as shown in Table 4 and Figure 4. Module A (score: 23.33) contained 25 nodes and 280 edges. All of the genes in

module A were downregulated, and the top five were *Cdk1*, *Ccnb1*, *Cdc20*, *Mad2l1*, and *Ccna2*. Module B (score: 5.24) contained 22 nodes and 55 edges (Figure 3). Most genes in this module were upregulated except for *Colla1* and *Cyr61*.

Function analysis of module genes

Genes in module A were significantly enriched in six KEGG pathways, including cell cycle, DNA replication, oocyte meiosis, progesterone-mediated oocyte maturation, and foxo signaling pathway. For GO BP, microtubule-based movement, mitotic cell cycle, cell

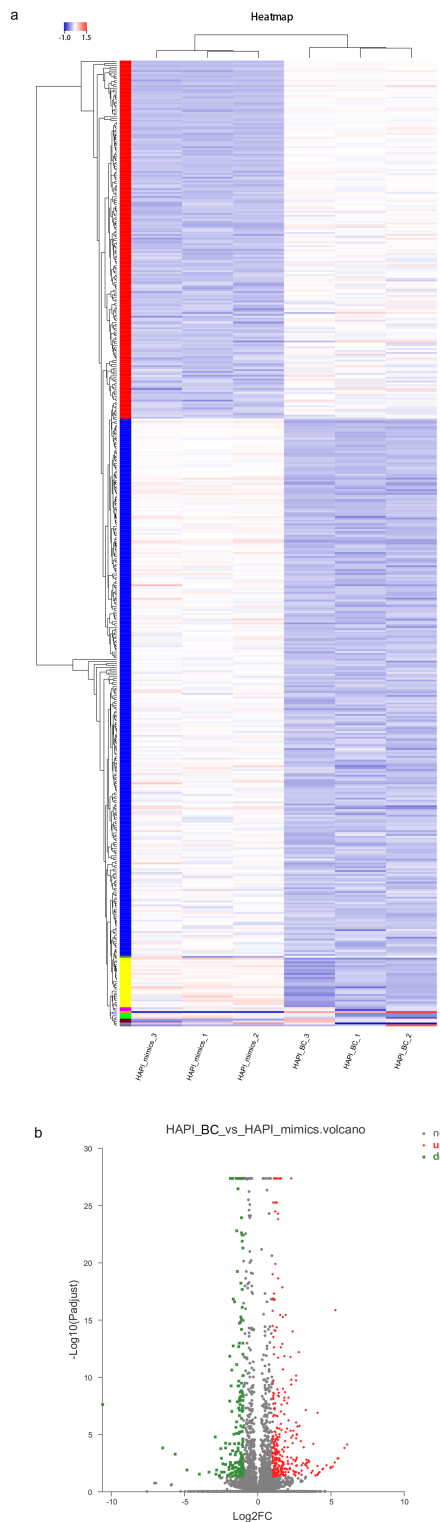


Figure 2. The heatmap (a) and volcano plot (b) of differentially expressed genes.

division, and DNA unwinding involved in DNA replication terms were significantly enriched. The top five BP terms of module B were anterior/posterior pattern specification, embryonic skeletal system morphogenesis, embryonic skeletal system development, positive

Table 3. Pathways and BP terms (top 5) enriched by down-regulated DEGs.

Category	Term	Count	PValue
PATHWAY	rno04110:Cell cycle	11	4.31E-07
PATHWAY	rno03030:DNA replication	6	2.16E-05
PATHWAY	rno04914:Progesterone-mediated oocyte maturation	6	2.11E-03
PATHWAY	rno04114:Oocyte meiosis	6	6.59E-03
PATHWAY	rno03008:Ribosome biogenesis in eukaryotes	5	1.07E-02
GO_BP	GO:1902975~ mitotic DNA replication initiation	4	1.10E-05
GO_BP	GO:0006268~ DNA unwinding involved in DNA replication	5	2.96E-05
GO_BP	GO:0045944~ positive regulation of transcription from RNA polymerase II promoter	26	3.90E-05
GO_BP	GO:0000727~ double-strand break repair via break-induced replication	4	1.16E-04
GO_BP	GO:0045893~ positive regulation of transcription, DNA-templated	17	3.32E-04

regulation of transcription from RNA polymerase II promoter, and cellular response to hormone stimulus.

Transcription factor (TF)-target and miRNA-target networks

In total, 6 TFs were predicted for the module genes, involving 58 pairs of TF-target regulatory relationships. As shown in Figure 5(a), the six TFs were NFY, NFAT, GFI1, PAX4, HNF1, and GER1. NFY had the highest degree, which regulated the most target genes, such as the downregulated genes of *Ncapd2*, *Ube2c*, *Pola1*, *Ccna2*, *Cdk1*, *Mcm4*, etc., and upregulated genes of *Rhoq*, *Stat3*, *Pbx2*, etc. GFI1, NFAT, PAX4, and EGR1 regulated eight target genes, respectively. HNF1 regulated seven target genes. The downregulated gene of *Col1a1* was regulated by four TFs, including NFY, NFAT, PAX4, and HNF1.

Based on the module genes, 17 miRNAs were predicted, such as MIR106A, MIR106B, MIR20B, and MIR519D. The miRNA-target network was conducted, which included 17 miRNAs and 18 genes (five downregulated and 13 upregulated), involving 99 regulatory relation pairs (Figure 5(b)). Among the 18 genes, *Pbx1*, *Pbx2*, and *Col1a1* were the center nodes with degrees greater than 10. In addition, *Arhgef12*, *Rhoc*, *Kif23*, and *Stat3* also showed high connectivity degrees with the miRNAs.

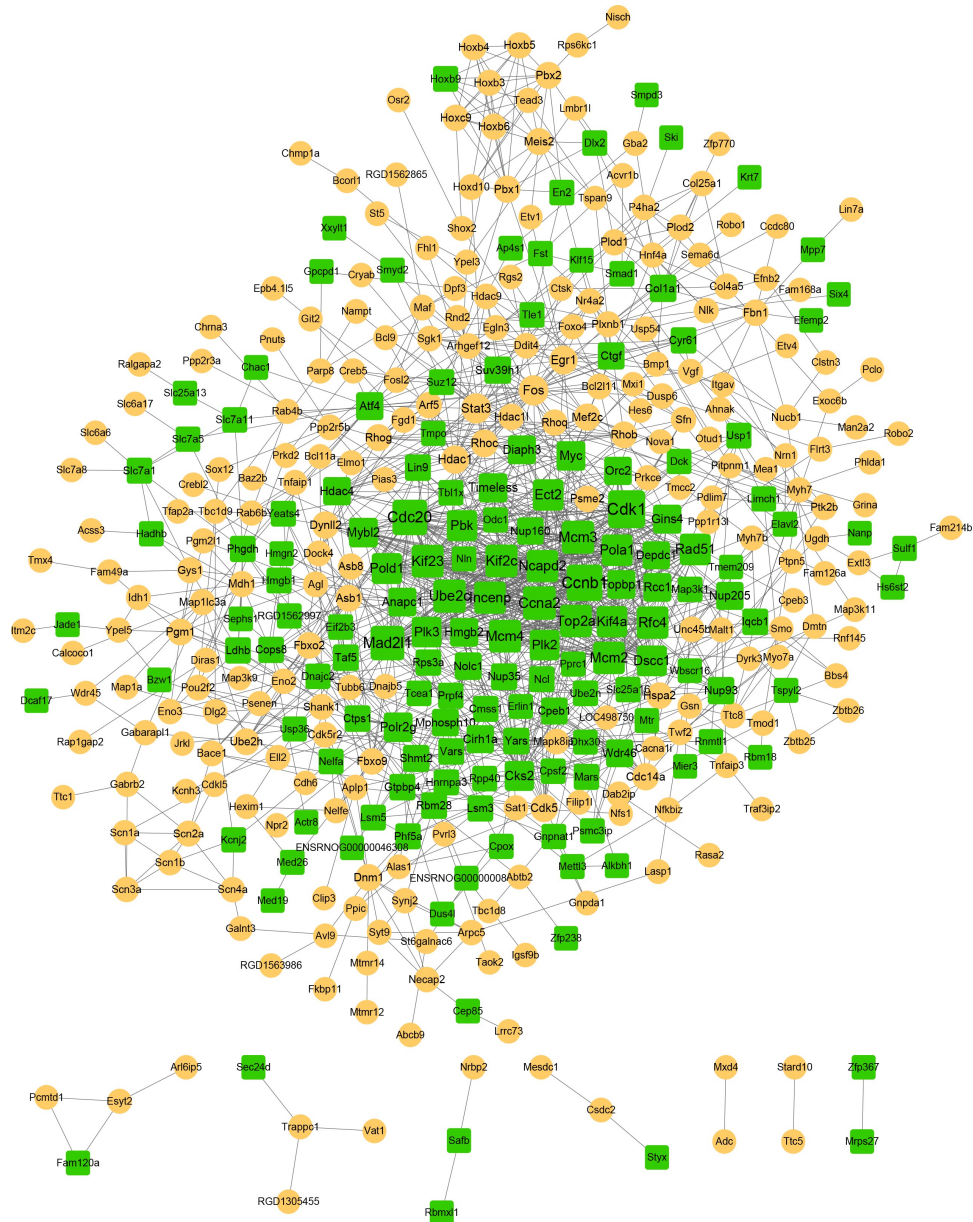


Figure 3. The constructed PPI network. The yellow circle represents upregulated gene, and the green square represents downregulated gene. The size of the node is based on the degree value, with higher degree values indicated by larger nodes.

Verification of differentially expressed genes (DEGs) by qPCR and western blotting

Efferocytosis-related genes, *Slc7a5*, *Rhog*, *Smad1*, *Rhog*, and *Mybl2*, were selected from DEGs and their expression levels were verified by qPCR and western blotting. As shown in Figure 6(a), the mRNA expression levels of *Slc7a5*, *Rhog*, and *Smad1* were significantly different between the two groups. After that, the protein levels of *Slc7a5* and *Rhog* were detected by western blotting. As shown in Figure 6(b), *Slc7a5* was significantly

downregulated, while *Rhog* was significantly upregulated in the miR-33-5p mimic group.

Discussion

In this study, gene expression data were analyzed to identify genes involved in microglia upon over-expression of miR-33-5p. Compared with the control groups, 507 DEGs were identified in groups with mimics. *Cdk1*, *Ccnb1*, and *Cdc20* had higher degrees in the PPI module. TFs of *NFY*, *NFAT*,

Table 4. Genes in module-A and module-B.

module-A			module-B		
Nodes	Description	Degree	Nodes	Description	Degree
Cdk1	down	55	Stat3	up	24
Ccnb1	down	49	Egr1	up	18
Cdc20	down	45	Rhoc	up	14
Mad2l1	down	41	Pbx1	up	12
Ccna2	down	37	Col1a1	down	12
Ube2c	down	36	Pbx2	up	11
Mcm3	down	35	Rhog	up	11
Kif23	down	34	Rhob	up	10
Mcm4	down	34	Hoxc9	up	9
Kif2c	down	34	Plod1	up	8
Top2a	down	33	Rhoq	up	8
Mcm2	down	33	Cyr61	down	8
Rfc4	down	33	Hoxb6	up	8
Incenp	down	32	Hoxb5	up	8
Ncapd2	down	32	Hoxb3	up	7
Rad51	down	30	Plod2	up	7
Ect2	down	29	Hoxb4	up	7
Pola1	down	29	P4ha2	up	6
Kif4a	down	28	Fgd1	up	6
Pold1	down	27	Col4a5	up	6
Pbk	down	27	Arhgef12	up	6
Dsccl	down	26	Col25a1	up	5
Plk3	down	25			
Plk2	down	25			
Cks2	down	23			

GFI1, *PAX4*, *HNF1*, and *GER1* had regulatory relationships with the DEGs.

The differential expression of *Slc7a5* and *Rhog* and the proteins encoded by them was verified by RT-PCR and western blotting, respectively. *Slc7a5* plays a critical role in cell growth and proliferation [29]. To our knowledge, this is the first report to

demonstrate the regulatory relationship between miR-33-5p and *Slc7a5*. There is convincing evidence that *Slc7a5* is deeply involved in the occurrence of ischemic stroke [30]. Therefore, more detailed studies are needed to prove the regulatory relationship between *Slc7a5* and miR-33-5p. *Rhog* is a member of the Rho family, which plays an important role in regulating cytoskeletal reorganization in physiological and pathophysiological situations [31]. To our best knowledge, there was no report about the associations between *Rhog* and miR-33-5p or ischemic stroke; therefore, we hypothesized that *Rhog* might participate in M1/M2 polarization based on our results.

All the genes in module A were downregulated. Among the 25 genes in module A, *Cdk1*, *Ccnb1*, and *Cdc20* possessed the most interactions with other genes. Cyclin-dependent kinases (*Cdks*) have already been reported to mediate the death of ischemic neuronal cells. Zhang et al. proved that the expression of *Cdk1* was induced when primary cortical neuron cultures were exposed to oxygen–glucose deprivation (OGD) for 4 h [32]. *Cdk1* also showed partial resistance to OGD-induced neuronal cell death [33]. Moreover, *Cdk1* has also been shown to play a critical role in neuronal death and has been reported to contribute to the pathogenesis of neurodegenerative diseases [34]. Currently, it

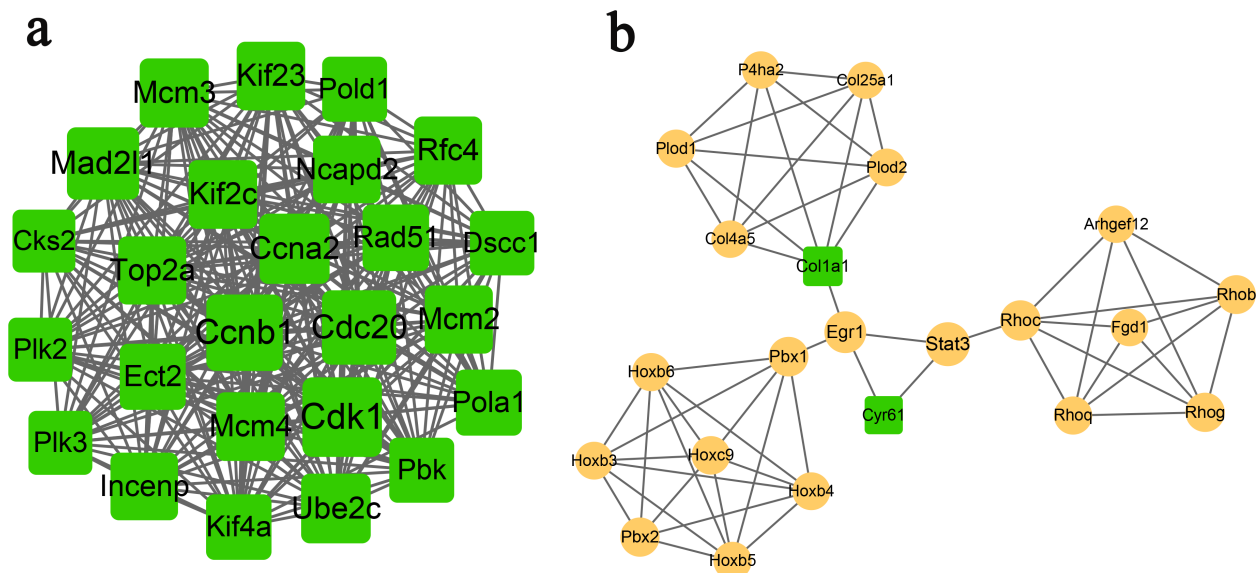


Figure 4. Subnetworks (a, module-A; b, module-B) of PPI network. Yellow circles indicate upregulated genes, and green squares indicate downregulated genes. The size of a node is based on the degree value, with higher degree values indicated by larger nodes.

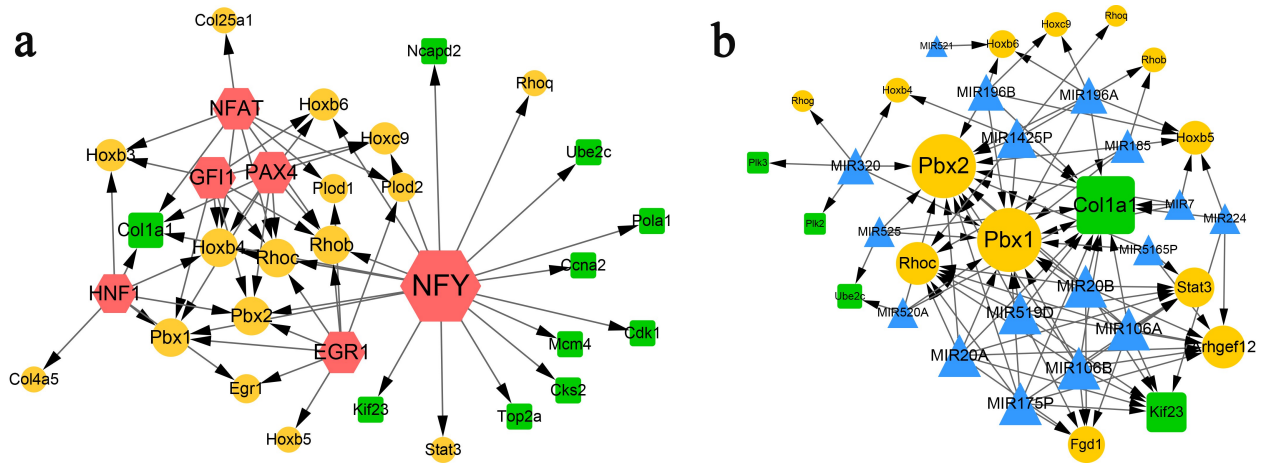


Figure 5. TF-target (a) and miRNA-target (b) networks. Yellow circles indicate upregulated genes. Green squares indicate downregulated genes. Blue triangles indicate predicted miRNAs. Red hexagons indicate transcription factors.

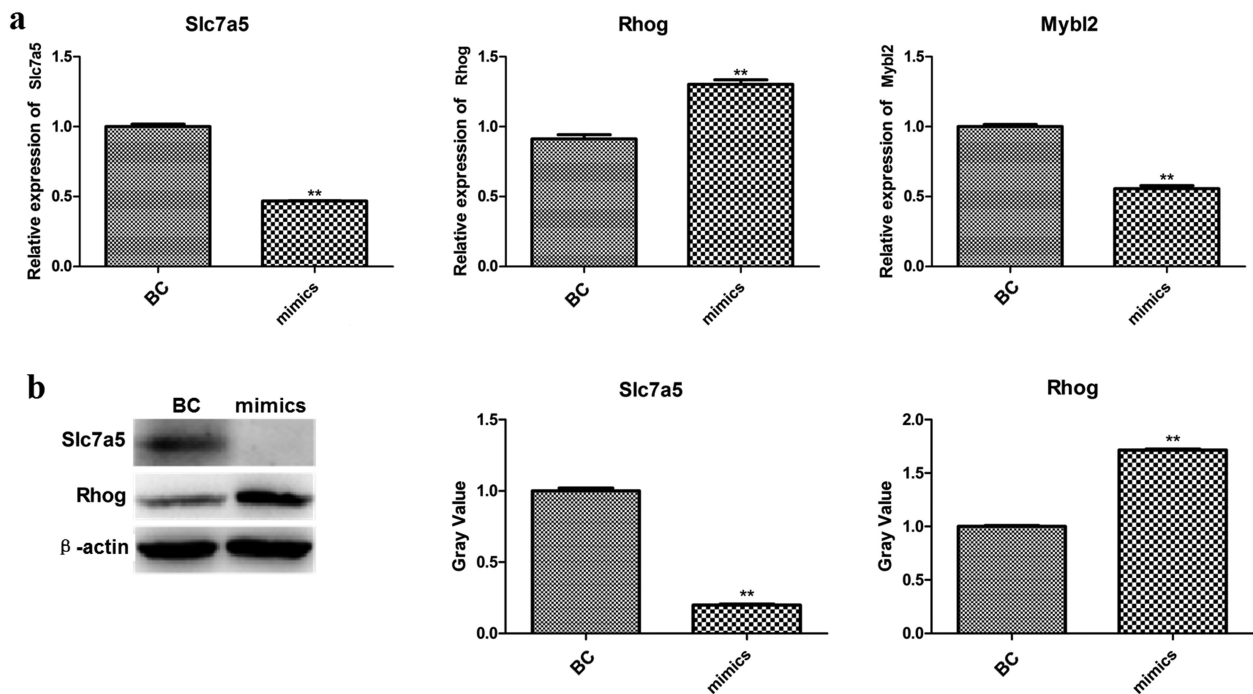


Figure 6. The mRNA (a) and protein levels (b) of verified genes.

is generally accepted that *Cdk1* regulates the cell cycle. Importantly, miR-33 has been demonstrated to play a crucial role in cell proliferation and cell cycle progression by modulating the expression of *Cdk1* [35,36]. Our results were consistent with the abovementioned studies, indicating that the interactions between miR-33 and *Cdk1* may affect the development of ischemic stroke.

Cyclin B1 (*Ccnb1*), an important regulator of the cell cycle machinery, is essential for mouse

embryonic development [37]. Several studies have shown that *Ccnb1* is involved in central nervous system regeneration driven by microglia [38]. However, there was no evidence to prove the direct regulation between *Ccnb1* and miR-33-5p. *Cdc20* is an important cell-cycle regulator for the completion of mitosis in organisms [39]. Lloyd et al. found that *Cdc20* could promote the proliferation of microglia through its population replacement process [40]. Elevated *Cdc20* increased extensive mitotic errors, leading to chromosome

mis-segregation [41]. Based on the existing literature, we speculated that miR-33-5p may regulate the expression of genes involving in caryomitosis and cell cycle, such as *Cdk1*, *Ccnb1*, and *Cdc20*.

Interestingly, we found that collagen type I alpha I (*Col1a1*) appeared in module-B, TF-target, and miRNA-target networks. It has been reported that *Col1a1* is highly related to osteoporotic fracture [42], bone mineral density, and osteoporotic fracture [43]. The only research that associated *Col1a1* with ischemic stroke was completed by Choi et al., who investigated the changes in gene expression after ischemic stroke [44]. In our results, the TF of nuclear factor Y (NFY) showed a wide range of interactions with nine downregulated genes. NFY was proved to be associated with the sterol regulation of human fatty acid synthase promoter I [45]. However, no studies have identified the direct relationship between NFY and microglia or ischemic stroke. We hypothesize that NFY may be involved in microglial polarization by indirectly regulating other genes.

Conclusions

In conclusion, our result for the first time demonstrated that miR-33-5p plays a crucial role in the M1/M2 polarization of microglia. Overexpression of miR-33-5p induced a significant change in the expression of *Slc7a5* and *Rhog*. Genes that regulate neuron cell cycle and death, such as *Cdk1*, *Ccnb1*, and *Cdc20*, attracted our attention due to their high potential for M1/M2 polarization.

Authors' contributions

Bo Yu, Dingying Ma, and Wenhua Chen carried out the conception and design of the research and obtained the funding. Ran Sun, Fei He and Lihua Chen participated in data acquisition. Song Chai, Yilan Sheng, Fei He and Ran Sun participated in the data analysis, and interpretation. Yilan Sheng, Jieshi He and Lihua Chen performed the statistical analysis. Song Chai, Yilan Sheng, Bo Yu and Ran Sun drafted this paper. Bo Yu and Dingying Ma participated in the revision of the manuscript for important intellectual content. All authors have read and approved the final manuscript.

Availability of data and materials

The data that support the findings of this study are available from the corresponding author upon reasonable request.

Disclosure statement

No potential conflict of interest was reported by the author(s).

Funding

This study was supported by the program of Shanghai Science and Technology Committee (No.20S31905600), Ningbo Medical Science and Technology Plan Project (No.2021Y36) and Scientific Research and Innovation Team Funding Plan of Shanghai Sanda University.

References

- [1] Wei H, Li H, Song X, et al. Serum klotho: a potential predictor of cerebrovascular disease in hemodialysis patients. *BMC Nephrol.* 2019;20(1):63.
- [2] Sudlow C, Martínez González NA, Kim J, et al. Does apolipoprotein E genotype influence the risk of ischemic stroke, intracerebral hemorrhage, or subarachnoid hemorrhage? Systematic review and meta-analyses of 31 studies among 5961 cases and 17 965 controls. *Stroke.* 2006;37(2):364–370.
- [3] Tsvigoulis G, Katsanos AH, Patousi A, et al. Stroke recurrence and mortality in northeastern Greece: the Evros Stroke Registry. *J Neurol.* 2018;265(10):2379–2387.
- [4] Leonard B, Maes MJN, Reviews B. Mechanistic explanations how cell-mediated immune activation, inflammation and oxidative and nitrosative stress pathways and their sequels and concomitants play a role in the pathophysiology of unipolar depression. *Neuroscience and Biobehavioral Reviews.* 2012;36(2):764–785.
- [5] Tang Y, Le W. Differential roles of M1 and M2 microglia in neurodegenerative diseases. *Molecular Neurobiology.* 2016;53(2):1181–1194.
- [6] Galli SJ, Borregaard N, TAJNi W. Phenotypic and functional plasticity of cells of innate immunity: macrophages, mast cells and neutrophils. *Nature Immunology.* 2011;12(11):1035.
- [7] Brierley J, Brown Ajjo CN. The origin of lipid phagocytes in the central nervous system: i. The intrinsic microglia. *The Journal of Comparative Neurology.* 1982;211(4):397–406.
- [8] CJJJJoAsdr C. Genetic, transcriptome, proteomic, and epidemiological evidence for blood-brain barrier disruption and polymicrobial brain invasion as determinant factors in Alzheimer's disease. *Journal of Alzheimer's disease reports.* 2017;1:125–157.
- [9] Ponomarev ED, Veremeyko T, Hljg W. MicroRNAs are universal regulators of differentiation, activation, and polarization of microglia and macrophages in normal and diseased CNS. *Glia.* 2013;61(1):91–103.
- [10] Orihuela R, McPherson CA, GJJBjop H. Microglial M1/M2 polarization and metabolic states. *British Journal of Pharmacology.* 2016;173(4):649–665.



- [11] Dey R, Sultana S, BJJon B. Combination treatment of celecoxib and ciprofloxacin attenuates live *S. aureus* induced oxidative damage and inflammation in murine microglia via regulation of cytokine balance. *Journal of Neuroimmunology*. 2018;316:23–39.
- [12] Iadecola C, JjNm A. The immunology of stroke: from mechanisms to translation. *Nature Medicine*. 2011;17(7):796.
- [13] Jang E, Lee S, Kim J-H, et al. Secreted protein lipocalin-2 promotes microglial M1 polarization. *FASEB Journal: Official Publication of the Federation of American Societies for Experimental Biology*. 2013;27(3):1176–1190.
- [14] Chhor V, Le Charpentier T, Lebon S, et al. Characterization of phenotype markers and neurotoxic potential of polarised primary microglia in vitro. *Brain, Behavior, and Immunity*. 2013;32:70–85.
- [15] P-c H, Chang K-C, Chuang Y-S, et al. Cholesterol regulation of receptor-interacting protein 140 via microRNA-33 in inflammatory cytokine production. *FASEB Journal: Official Publication of the Federation of American Societies for Experimental Biology*. 2011;25(5):1758–1766.
- [16] Marquart TJ, Allen RM, Ory DS. Baldán ÁJPotnaos. miR-33 links SREBP-2 induction to repression of sterol transporters. *Proceedings of the National Academy of Sciences of the United States of America*. 2010;107(27):12228–12232.
- [17] Iwakiri YJCC. A role of miR-33 for cell cycle progression and cell proliferation. *Cell Cycle*. 2012;11:1057.
- [18] Zeng Y, Liu JX, Yan ZP, et al. Potential microRNA biomarkers for acute ischemic stroke. *International Journal of Molecular Medicine*. 2015;36(6):1639–1647.
- [19] Jan A, Karasinska JM, Kang MH, et al. Direct intracerebral delivery of a miR-33 antisense oligonucleotide into mouse brain increases brain ABCA1 expression. *Neuroscience Letters*. 2015;598:66–72.
- [20] Wang L, Zhang L, Chen Z-B, et al. Icaritin enhances neuronal survival after oxygen and glucose deprivation by increasing SIRT1. *European Journal of Pharmacology*. 2009;609(1–3):40–44.
- [21] Wang G. P50-M high-throughput and automatic plasmid DNA preparation with SeqPrep technology. *Journal of Biomolecular Techniques: JBT*. 2007; 18 (1): 17 .
- [22] Joshi N, Fass J. Sicklet: a sliding-window, adaptive, quality-based trimming tool for FastQ files (Version 1.33)[Software]. 2011.
- [23] Kim D, Pertea G, Trapnell C, et al. TopHat2: accurate alignment of transcriptomes in the presence of insertions, deletions and gene fusions. *Genome Biology*. 2013;14(4):R36.
- [24] Trapnell C, Roberts A, Goff L, et al. Differential gene and transcript expression analysis of RNA-seq experiments with TopHat and Cufflinks. *Nature Protocols*. 2012;7(3):562–578.
- [25] Pertea M, Pertea GM, Antonescu CM, et al. StringTie enables improved reconstruction of a transcriptome from RNA-seq reads. *Nature Biotechnology*. 2015;33(3):290.
- [26] Huang DW, Sherman BT, Lempicki RA. Systematic and integrative analysis of large gene lists using DAVID bioinformatics resources. *Nat Protocols*. 2008;4(1):44–57.
- [27] Mering C, Huynen M, Jaeggi D, et al. STRING: a database of predicted functional associations between proteins. *Nucleic acids research*. 2003;31:258–261.
- [28] Liao Y, Wang J, Jaehnig EJ, et al. WebGestalt 2019: gene set analysis toolkit with revamped UIs and APIs. *Nucleic Acids Res*. 2019;47(W1):W199–W205.
- [29] Yanagida O, Kanai Y, Chairoungdua A, et al. Human L-type amino acid transporter 1 (LAT1): characterization of function and expression in tumor cell lines. *Biochim Biophys Acta*. 2001;1514(2):291–302.
- [30] Tornabene E, Brodin B. Stroke and Drug Delivery–In Vitro Models of the Ischemic Blood-Brain Barrier. *J Pharm Sci*. 2016;105(2):398–405.
- [31] Schumacher S, Franke K. miR-124-regulated RhoG: a conductor of neuronal process complexity. *Small GTPases*. 2013;4(1):42–46.
- [32] Zhang B, Kirov S, JJNar S. WebGestalt: an integrated system for exploring gene sets in various biological contexts. *Nucleic Acids Research*. 2005;33(Web Server issue):W741–W8.
- [33] Marlier Q, Jibassia F, Verteneuil S, et al. Genetic and pharmacological inhibition of Cdk1 provides neuroprotection towards ischemic neuronal death. *Cell death discovery*. 2018;4:1–12.
- [34] Kim AH, Ajcc B. Cdk1-FOXO1: a mitotic signal takes center stage in post-mitotic neurons. *Cell Cycle (Georgetown, Tex.)*. 2008;7(24):3819–3822.
- [35] Cirera-Salinas D, Pauta M, Allen RM, et al. Mir-33 regulates cell proliferation and cell cycle progression. *Cell Cycle (Georgetown, Tex.)*. 2012;11(5):922–933.
- [36] Salinas DC. miR-33 regulates cell proliferation, cell cycle progression and liver regeneration. Berlin, Humboldt Universität zu Berlin, Diss. . 2013.
- [37] Tang J-X, Li J, Cheng J-M, et al. Requirement for CCNB1 in mouse spermatogenesis. *Cell Death & Disease*. 2017;8(10):e3142–e.
- [38] Lloyd AF, Davies CL, Holloway RK, et al. Central nervous system regeneration is driven by microglia necroptosis and repopulation. *Nature Neuroscience*. 2019;22(7):1046–1052.
- [39] HJMc Y. Cdc20: a WD40 activator for a cell cycle degradation machine *Molecular cell*. 2007;27:3–16.
- [40] Lloyd AF, Davies CL, Miron VE. Microglia: origins, homeostasis, and roles in myelin repair. *Current Opinion in Neurobiology*. 2017;47:113–120.
- [41] Godek KM, Kabeche L, Dajnrmb C. Regulation of kinetochore–microtubule attachments through homeostatic control during mitosis. *Nature Reviews. Molecular Cell Biology*. 2015;16(1):57–64.
- [42] Mann V, Hobson EE, Li B, et al. A COL1A1 Sp1 binding site polymorphism predisposes to osteoporotic fracture by affecting bone density and quality.

- The Journal of Clinical Investigation. 2001;107(7):899–907.
- [43] Mann V, Ralston SH. Meta-analysis of COL1A1 Sp1 polymorphism in relation to bone mineral density and osteoporotic fracture. Bone. 2003;32(6):711–717.
- [44] Choi I, Yun JH, Kim J-H, et al. Sequential Transcriptome Changes in the Penumbra after Ischemic Stroke. International journal of molecular sciences . 2019;20:6349.
- [45] Xiong S, Chirala SS, Wakil S. Sterol regulation of human fatty acid synthase promoter I requires nuclear factor-Y-and Sp-1-binding sites. Proceedings of the National Academy of Sciences of the United States of America. 2000;97(8):3948–3953.